International Journal of Infinite Innovations in Technology|ISSN:2278-9057
IJIIT|Volume-V|Issue-I|2016-2017 July|Paper-03
Reg. No.:20160603|DOI:V5I1P03

Signal Transmission by Galvanic Coupling Through the Human Body

Pravin Prakash Adivarekar, Singhania University, Rajasthan, India

ABSTRACT

Galvanic coupling is a promising approach for wireless intrabody data transmission between sensors. Using the human body as a transmission medium for electrical signals becomes a novel data communication technique in biomedical monitoring systems. In this paper, special attention is given to the coupling of the current into the human body. Safety requirements have to be fulfilled, and optimal signal coupling is of essence. Therefore, different electrodes are compared. A test system offers up to 1 mA contact current modulated in the frequency range of 10 kHz to 1 MHz. The injected current is up to 20 times below the maximum allowed contact current. Such a low-current approach enables data communication that is more energy saving than other wireless technologies.

Keywords:
Biomedical sensor network, electrode characterization, galvanic coupling, intrabody communication, measurement system.

I. INTRODUCTION

DATA transmission using the human body as a channel of electric near-field propagation is driven by the vision of a cable-free biomedical monitoring system. Wireless sensors give more freedom to patients and will revolutionize the possibilities in clinical monitoring. Data transfer by capacitive coupling through the human body was first proposed as a personal area network (PAN) [1]. It was discovered that certain parts of the near field could be exploited to make the human body act as a medium for data transmission.

The electric field, induced by a signal electrode of the PAN transmitter, passes through the body and flows toward the ground reference. Further systems with similar coupling methods have shown the potential of data communication through the human body [2]–[4]. All these systems used a fixed carrier frequency. The detector sensibility was increased by electrooptic sensors and extended in the signal frequency to above 1 MHz [5], [6].

The novel principle of galvanic coupling was investigated by Oberle [7] and was compared by Hachisuka et al. [8].

In comparison to capacitive coupling applying static charged electrode, galvanic coupling provides alternating currents over multiple electrodes. Two coupler electrodes induce currents into the human tissue and two detector electrodes sense the potential differences.

Ground is not required for reference as in the method of capacitive coupling. Electrical characterizations of the human body with respect to galvanic coupled current flow and identified differences between body parts are shown by Wegmueller et al. [9].

The feasibility of the technology has been proven, and its limits regarding tissue sensitivity and body geometry have been assessed. The exposure guidelines of the International Commission on Non-Ionizing Radiation Protection [10] are defined via maximum contact current and current density. State-ofthe-art intrabody communication transceiver units for usage in close body proximity have been developed for battery powered sensors.

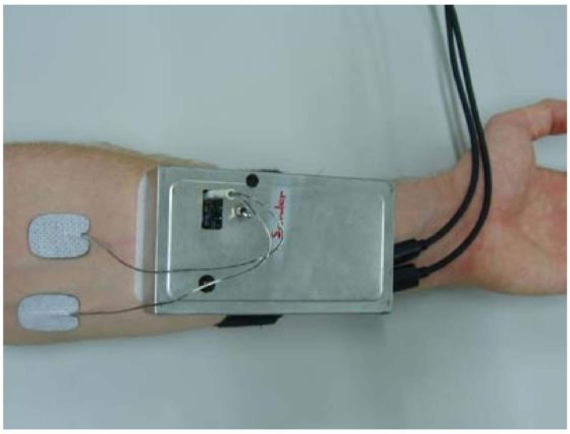

Fig. 1. Coupler unit attached to the lower arm using fixed gel electrodes.

However, comparison of different electrode types in the target frequency range has been missing, but the importance of optimal signal coupling became obvious and necessitated further investigation. In particular, there exist open points on the comparison of different electrode coupling materials and the size of the active electrode area. In this paper, advanced measurements with various coupling schemes are presented. Section II introduces the concept of galvanic coupling and a derived reference model.

The measurement hardware shown in Fig. 1 is described in Section III. Investigations over a wide range from 10 kHz to 1 MHz are enabled. Several electrodes are compared at the characteristic body parts identified in [11]. The measurements are discussed in Section IV, and conclusions are drawn in Section V.

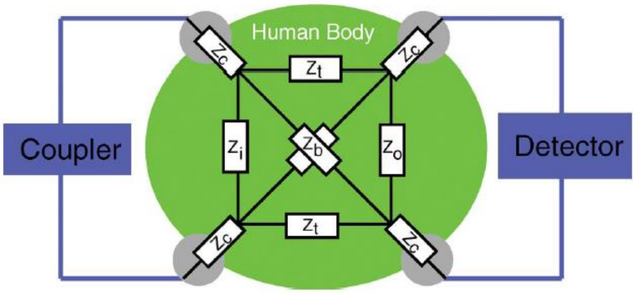

Fig. 2. Simplified circuit model of the human body modeling the coupling electrode impedances (Z_c), input impedances (Z_i), and output impedances (Z_o) as well as longitudinal transmit impedances (Z_t) and butterfly cross impedances (Z_b).

II. GALVANIC COUPLING

Galvanic coupling for intrabody communication denotes the technology of signal transmission through the body for onbody and implanted sensor communication. Thus, the human body becomes the transmission channel of the communication system. A profound understanding of its channel characteristics and the coupling impacts is required for defining the channel constraints and the subsequent system constraints of a transceiver design.

A. Concept of Transmission

Galvanic coupling follows the approach of coupling alternating current into the human body. The signal is applied differentially over two coupler electrodes and received differentially by two detector electrodes. The coupler establishes a modulated electrical field, which is sensed by the detector.

Therefore, a signal transfer is established between the coupler and detector units by coupling signal currents galvanically into the human body. The induced current has a peak amplitude of 1 mA, and the alternating signal frequency remains in the frequency range from 10 kHz to 1 MHz. The influence on body signals located below 10 kHz shall be omitted, while the drawback of signal loss above 1 MHz would be increasing.

B. Simplified Circuit Model of the Human Body

The goal of a simple discrete body model is the modeling of the main dependences on the skin layer and the coupling electrode conditions. The simple model shall reduce the body complexity to its minimum and shall be compared later with more detailed approaches.

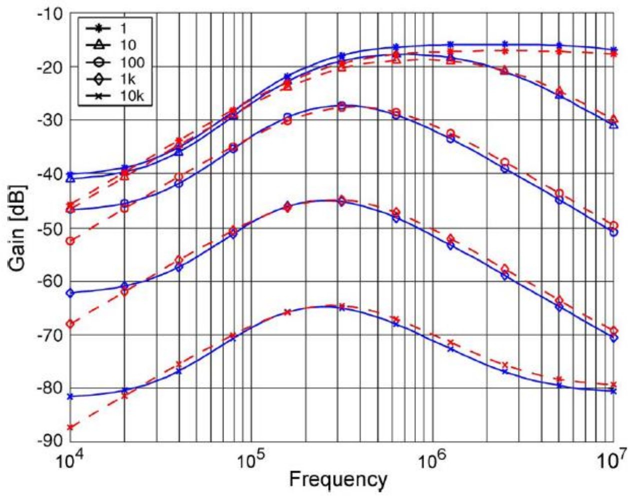

Fig. 3. Simulation results of the simplified (dashed) and complex (solid) tissue model with variance of the coupling resistances Z_c.

As shown in Fig. 2, intrabody transmission can be described by a four-terminal circuit model with ten complex impedances. This simplified model takes into account longitudinal transmit (Zt), input (Zi) and output impedances (Zo), as well as cross impedances (Zb) between coupler and detector electrodes. In a first approximation, the body impedances can be described as an equivalent parallel circuit of resistance Rp and capacitance Cp according to the Cole–Cole reference model [12].

The entire transfer function G includes the coupling electrode impedances (Zc), i.e.,

$$G = 20\ \log_{10}\left\{\frac{H}{1+Z_c\left[\frac{1}{Z_t}+\frac{1}{Z_b}+H\left(\frac{1}{Z_b}+\frac{1}{Z_i}-\frac{2}{Z_t}\right)\right]}\right\}. \quad (1)$$

Its characteristic is shown in Fig. 3 for different coupling impedances.

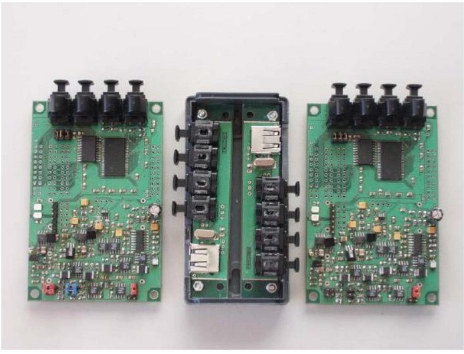

Fig. 4. Coupler, interface, and detector printed circuit board.

models have been applied [9], modeling up to three tissue layers (i.e., skin, muscle, and bone). For the finite-element simulations, 3-D elements and the simulations of the potential distribution were produced with the commercial package EMAG from ANSYS [13]. The simulations results of the complex model conform well with the simplified model in case of a simple geometrical structure like an arm, as shown in Fig. 3. Therefore, the simplified impedance model serves as model reference in this paper. It is sufficiently detailed for the transfer characteristic calculations and further allows fast estimation of coupling influences like the variances of electrode or skin contacts. For further investigations on more advanced body structures, full anatomical models will become a must.

C. Comparison With Complex Models

To learn more about the influence of the human anatomy on the signal propagation complex, layered and 3-D finite-element

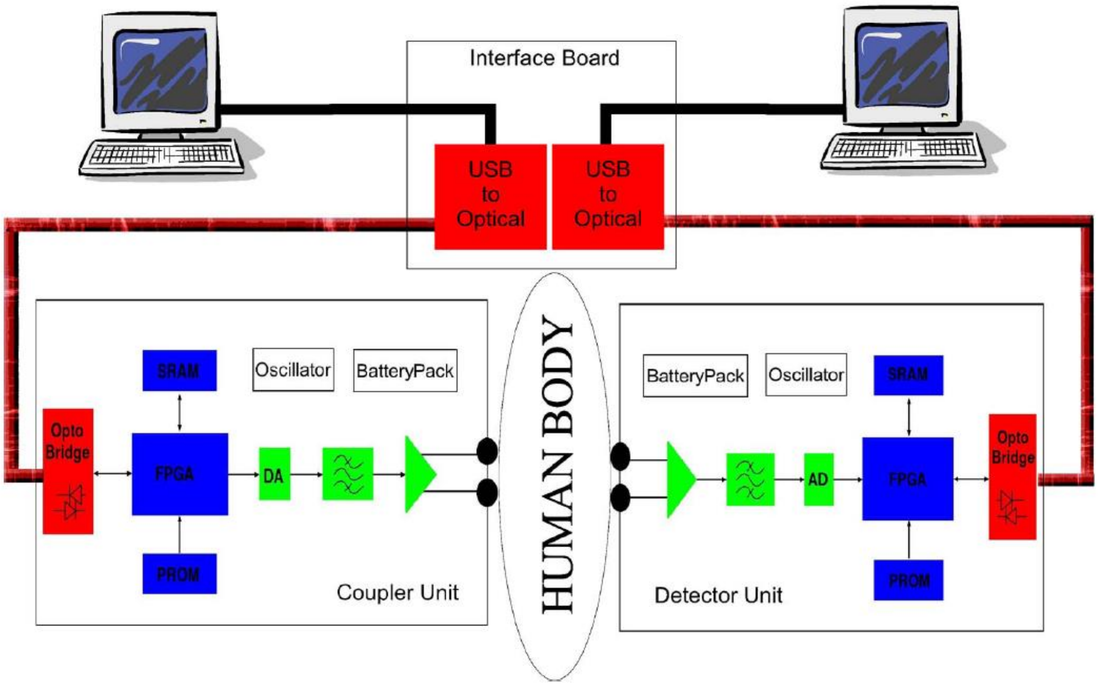

Fig. 5. Test system overview: coupler and detector units are optically connected by USB interface boards to host computers.

III. HARDWARE REALIZATION

Developed models and the simulation results regarding electrical signal transmission through the human body. Strict medical regulations have to be fulfilled for any system application on a human subject. To explore the concept of galvanic coupling, a sophisticated measurement system has been developed and approved by the Swiss National Advisory Commission on Biomedical Ethics (NEK-CNE).

A. System Architecture

The low-frequency measurement system is composed of two sensor units (i.e., coupler and detector) and an interface board (see Fig. 4). The interface board offers a serial optical connection to each of the two sensor units and universal serial bus (USB) interfaces to standard computers.

The coupler and detector units (Fig. 5) allow modulated electrical signal to be sent and received. A Xilinx SPARTAN IIE field-programmable gate array (FPGA) provides interfaces between an analog front end and the digital communication links.

TABLE I
ELECTRODE PROPERTIES COMPARING THE SIZE AND TYPE OF Swaromed, Neuroline, AND Blue Sensor ELECTRODES

Type	Active Area	Contact
Swaromed REF1008	80 mm^2	pre-gelled
Neuroline 715	54 mm^2	solid-gel
Blue Sensor BR	560 mm^2	solid-gel

The signals generated by the FPGA in the coupler are fed through a 12-bit digital-to-analog converter into a differential current output capable of a peak amplitude of 1 mA.

The coupling of the signal currents into the human tissue is performed through two electrodes attached to the skin (Fig. 1). The transmitted signals are differentially picked up by the detector electrodes and bandpass filtered. After an amplification of up to 72 dB, they are digitized by a 14-bit analog-to-digital converter at a sampling rate of 8 MSPS. Configuration and data collection are provided by bidirectional serial data links from each sensor to a host system. For measurement purposes, transmitted signals are recorded on both coupler and detector units. The recorded data are stored in an static random access memory and transferred over the serial optical link to the host system for further evaluation.

The serial optical data stream is converted to USB on the interface board. The host system initializes the sensors, starts the measurement, and collects the data for postprocessing. The basic functionality of the host is implemented in Perl using win32api libraries. Both coupler and detector units are battery powered and fully optically isolated. Therefore, the units are entirely electrically decoupled from any power lines and operate far below safety limits.

B. Electrode Types

The envisioned application requires flat and self-adhesive electrodes with a low contact resistance. Based on a survey of available electrodes and electrode technologies, the following products have been selected for further investigations (Table I; Fig. 6).

1) Swaromed REF 1008 ECG electrodes are pregelled and have a silver/silver chloride sensor.

Fig. 6. (1) *Swaromed REF 1008*. (2) *Neuroline 715*. (3) *Blue Sensor BR*.

TABLE II
CHARACTERISTIC BODY POINTS FOR COUPLING COMPARISON

Session	Coupler	Detector
Arm	B1 (elbow)	B2 (axillary)
Thorax	C1 (left)	E1 (right)

2) The Neuroline 715 electrode features a high-quality silver/silver chloride sensor. The transparent electrode area enables very precise location of the application position. The electrode is coated with a skin-friendly solid gel that allows repositioning several times without losing adhesive power.

3) The Blue Sensor BR features a skin-friendly solid gel that enables high signal quality and allows the electrode to be repositioned if necessary. Due to the cloth backing material, the skin is able to breathe such that the electrode remains comfortable to wear over long periods.

IV. BODY MEASUREMENTS

The measurement system is used for investigation of the transmission and coupling characteristics among subjects in a feasibility study conducted at the University Hospital Berne. Two volunteers have been chosen for the comparison of the electrode types. The selection of volunteers, measurement points, and electrode samples had been based on the study protocol jointly developed by the cardiology research group and the authors.

The volunteers had to stand still during the measurements of electrode comparison. Further investigations with different conditions (e.g., the impact of body structure, physiological parameters, geometry, and moisture on the performance) are shown in [9].

A. Test Strategy

In the trial, distinct differences between extremity and thorax measurements were identified. Based on these results, the following two setups as typical characteristics for either thin (e.g., extremities) or voluminous body parts were chosen for comparison of the various coupling strategies (Table II, Fig. 7):

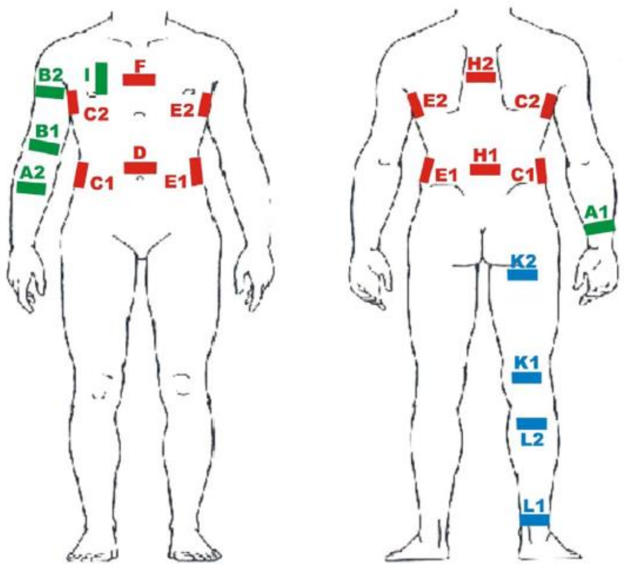

Fig. 7. Measurement point distribution over the entire body.

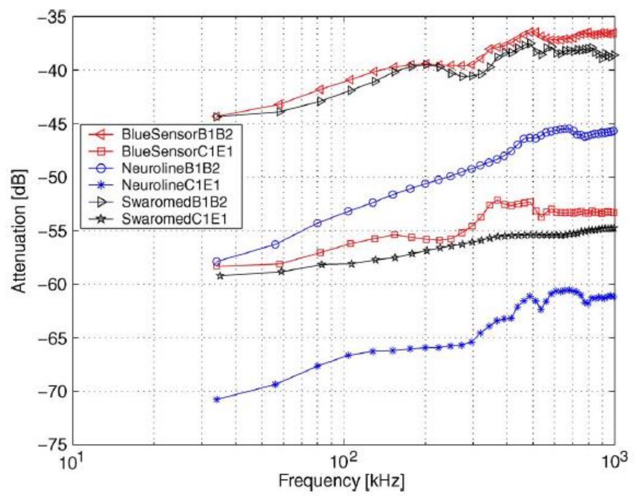

Fig. 8. Attenuation of different electrodes compared at body points on the upper arm from elbow B1 to axillary B2 and on the thorax C1 to E1.

1) on the upper arm: from elbow B1 to axillary B2;
2) on the thorax: from left C1 to right body side E1.

The measurement sensors were attached to the human body, as shown in Fig. 1. Both transmitter electrodes were attached with 5-cm spacing, while the receiver electrodes were separated by 7 cm or less, depending on the body geometry. Transmission on the arm is very sensitive to distance and location of attachment.

It follows a low-pass characteristic on the lower arm, whereas transmission on the thorax is rather constant with frequency. Results of further body part measurements are presented in [11].

To assess the coupling characteristics of the different electrodes at various locations, the following test strategies have been defined:

1) assessment of the signal attenuation between coupler and detector electrodes by sweeping a sinusoidal signal over the defined frequency range;
2) measurement of the coupling impedances with an induced signal current of 1 mA and frequencies of 100 kHz and 1 MHz.

B. Electrode Comparison

Fig. 8 shows the measured attenuation of all three electrode types. The Blue Sensor and Swaromed electrodes show rather similar attenuation in both setups on the upper arm (from elbow B1 to axillary B2) and on the thorax (C1 to E1). Swaromed electrodes behave on the upper arm with the absolute lowest attenuation.

The Neuroline electrode has the highest attenuation. When taking the much smaller contact areas into account, however, the Neuroline electrode is competitive with the Blue Sensor. In Table III, the measured impedances averaged over five experiments for every setup of the three electrode types are compared for the three locations, namely, Direct, B1, and C1. Direct indicates measurements with two electrodes pasted together.

That implies shorted Zi in Fig. 2; therefore, twice Zc is measured. In addition, the values of the input impedance measured at locations B1 and C1 are listed. The measurements were performed at 100 kHz and 1 MHz. The body input impedance (Zi in Fig. 2) is in the range of a few hundred ohms. In the case of the Neuroline at 1 MHz, the electrode resistance is in the range of the body resistance of approximately 200 Ω. Swaromed electrodes feature a significantly lower impedance. At 100 kHz, the body resistance is significantly higher with more than 300 Ω. In addition, different sizes of Blue Sensor electrodes have been compared. The active area was cut into one-half and one-quarter of the original size. The measured impedance values are shown in Table IV.

The smaller the size of the electrode is, the larger the resistance and the smaller the capacitance of the electrode will be. Thus, larger electrodes improve the transmission characteristics. However, for the envisioned application and a further miniaturization, a tradeoff has to be found.

In Fig. 9, the attenuation measurements with combinations of different coupler and detector electrode sizes are shown. The size of the detector electrodes has a negligible impact (results with index 44 compared to 41), whereas the attenuation decreases with an increase in size of the coupler electrodes (41, 21, down to 11).

The influence of the coupler electrodes has been confirmed in the finite-element model simulations, as shown in Fig. 9. A doubling in the size of the coupler electrodes caused a lower attenuation of 6 dB in the simulations. In summary, the comparison between Swaromed REF1008, Neuroline 715, and Blue Sensor BR has shown the following.

1) Electrodes with a lower resistance led to a lower attenuation and, therefore, feature a longer transmission.

2) Pregelled Swaromed electrodes feature a lower coupling resistance compared to solid–gel electrodes, e.g., Neuroline.

3) Solid–gel electrodes with lower capacitive values are superior to the pregelled electrodes. Both the electrode impedance and the electrode-skin impedance can increase up to the kiloohm range.

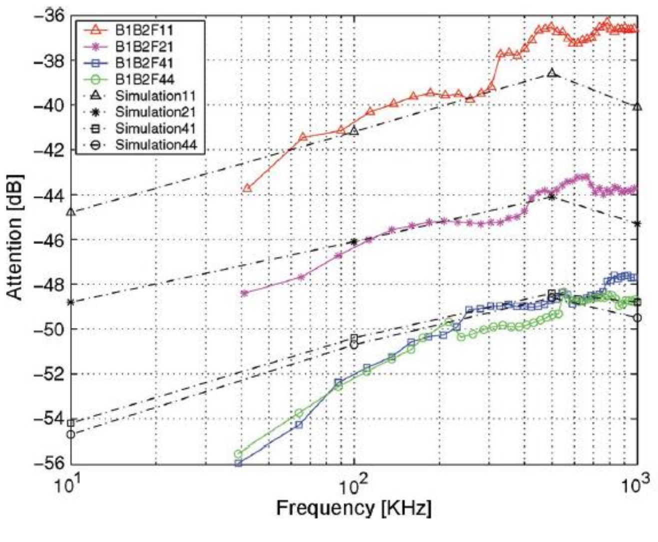

Fig. 9. Measurement and simulation results: attenuation on the upper arm B1 to B2 with different sizes of *Blue Sensor* electrodes (11: coupler and detector 560 mm^2; 21: coupler 280 mm^2 and detector 560 mm^2; 41: coupler 140 mm^2 and detector 560 mm^2; and 44: coupler and detector 140 mm^2).

This causes a huge undesired loss, as seen in Fig. 8, and coupling problems become clear with a high electrode impedance for the resistive and the capacitive parts. Therefore, the electrode impedances have to be minimized.

C. Transmission Channel Performance

The channel behavior is characterized by the signal-to-noise ratio (SNR), as defined in accordance with Shannon [14], as the ratio between the total transmitted power and the noise power. The channel capacity is defined according to Shannon by the signal bandwidth (BW) and the SNR as

$$C = BW \cdot \log2(1 + SNR).$$

The parameters for the measurements on the upper arm and the thorax are indicated in Table V.

The feasibility measurements have shown that the novel technology has the potential to transmit data through the human body by galvanic coupling. The signal attenuation is highly dependent on the coupling electrodes and the application location.

1) The upper arm has been identified as the body part with the best performance. This short-range transmission features a low attenuation of 40 dB, a high SNR of 37 dB, and a high resulting channel capacity of 1.23 Mb/s.

2) The thorax showed stable attenuation independent of the location. Compared with the upper arm, a higher attenuation and a lower SNR were measured. The findings shall be confirmed and extended further among a set of subjects by applying the system in a clinical study.

D. Uncertainty Consideration

Major causes of uncertainty are thermal noise at the receiver input, body impedance variations (tissue state, e.g., wet and dry), electrode coupling (considered electrode and its measurement contact), and the precision of the measurement hardware. The contact impedance variations are dominant. The variations result in part from the electrode skin contact, the alignment of the electrodes, and the dependency on contact pressure. Standard deviations up to 26% have been observed for the measured resistance. Attenuation variations of up to 6 dB are determined between experiments at rest and during ergo meter exposure. The minor uncertainty of the instrument was validated with comparable impedances in a laboratory setup.

V. CONCLUSION

Galvanic coupling is a promising approach for intrabody communication. The versatile platform presented here offers sophisticated possibilities for signal application and data transmission using a differential pair of electrodes that are galvanically coupled to the human body.

Different electrodes were compared with the proposed measurement system. Pregelled Swaromed electrodes feature lower coupling resistances compared to solid–gel electrodes. Nevertheless, solid–gel electrodes with lower capacitive values are superior to pregelled electrodes.

With application-specific electrodes, the technology is enhanced. The proposed system will be miniaturized with the goal of realizing data transmission based on galvanic coupling in a biomedical system for monitoring vital functions.

VI. FUTURE SCOPE

If all PCs are connected on the conference table then it will be able to transmit the data over all the PCs at the same time as shown in figure.

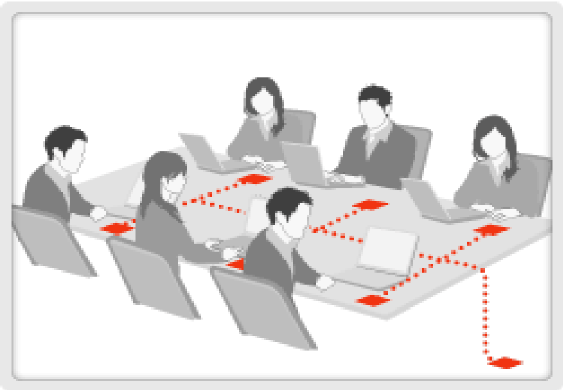

By handshaking it will be able to transmit the data between two devices which is carried by the humans as shown in figure

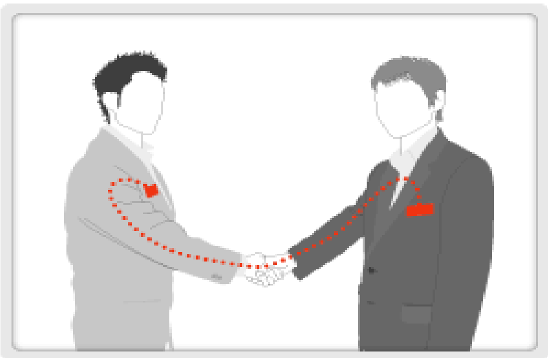

By installing the designed system in the printer and touching the printer simultaneously with mobile device it will be able to print the document as shown in fig.

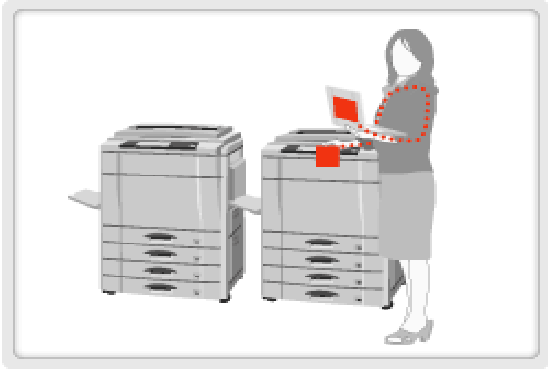

Further the rapid increase in healthcare demand has also seen novel developments in health monitoring technologies such as body area network (BAN) paradigm. BAN technology consists of a network of sensors which operates continuously and measure critical physical and physiological parameters like mobility, heart rate and glucose level. So the Intrabody communication is an alternative option in BAN.

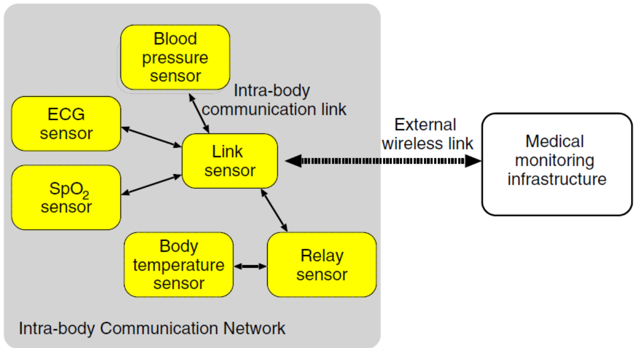

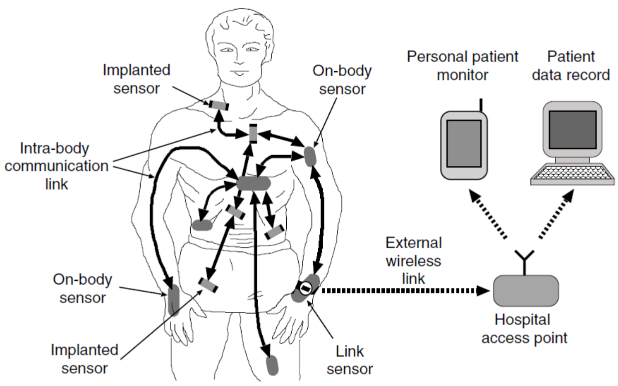

REFERENCES

[1] T. G. Zimmerman, "Personal Area Network (PAN)," M.S. thesis, MIT Press, Cambridge, MA, 1995.

[2] T. Handa, S. Shoji, S. Ike, S. Takeda, and T. Sekiguchi, "A very lowpower consumption wireless ECG monitoring system using body as a signal transmission medium," in Proc. Int. Conf. Transducers, Solid-State Sensors Actuators, 1997, pp. 1003–1007.

[3] K. Partridge, B. Dahlquist, A. Veiseh, A. Cain, A. Foreman, J. Goldberg, and G. Borriello, "Empirical measurements of intrabody communication performance under varied physical configurations," in Proc. ACM UIST, 2001, pp. 183–190.

[4] K. Fujii, M. Takahashi, K. Ito, K. Hachisuka, Y. Terauchi, Y. Kishi, and K. Sasaki, "A study on the transmission mechanism for wearable devices using the human body as a transmission channel," IEICE Trans. Commun., vol. E88-B, no. 6, pp. 2401–2410, Jun. 2005.

[5] M. Shinagawa, M. Fukomoto, K. Ochiai, and H. Kyruagi, "A near-fieldsensing transceiver for intra-body communication based on the electrooptic effect," in Proc. IMTC, 2003, pp. 296–301.

[6] A. Sasaki, M. Shingawa, and K. Ochiai, "Sensitive and stable electrooptic sensor for intrabody communication," in Proc. LEOS, 2004, vol. 1, pp. 122–123.

[7] M. Oberle, "Low power system-on-chip for biomedical application," Ph.D. dissertation, IIS/ETH Zurich, Zurich, Switzerland, 2002.

[8] K. Hachisuka, Y. Terauchi, Y. Kishi, T. Hirota, K. Sasaki, H. Hosaka, and K. Ito, "Simplified circuit modeling and fabrication of intrabody communication devices," in Proc. 13th Int. Conf. Solid-State Sensors, Actuators Microsyst., 2005, vol. 2E4-3, pp. 461–464.

[9] M. S. Wegmueller, A. Kuhn, J. Froehlich, M. Oberle, N. Felber, N. Kuster, and W. Fichtner, "An attempt to model the human body as a communication channel," IEEE Trans. Biomed. Eng., vol. 54, no. 10, pp. 1851–1857, Oct. 2007.

[10] Int. Commission Non-Ionizing Radiation Protection (ICNIRP), Guidelines for Limiting Exposure to Time-Varying Electric, Magnetic, and Electromagnetic Fields (up to 300 GHz), Oberschleissheim, Germany, 1997.

[11] M. Wegmueller, A. Lehner, J. Froehlich, R. Reutemann, M. Oberle, N. Felber, N. Kuster, O. Hess, and W. Fichtner, "Measurement system for the characterization of the human body as a communication channel at low frequency," in Proc. IEEE EMBC, Shanghai, China, 2005, pp. 3502–3505.

[12] K. S. Cole and R. H. Cole, "Dispersion and absorption in dielectrics— Part 1: Alternating current characteristics," J. Chem. Phys., vol. 9, no. 4, pp. 341–351, Apr. 1941.

[13] EMAG From ANSYS. [Online]. Available: www.ansys.com

[14] C. E. Shannon, "A mathematical theory of communication," Bell Syst. Tech. J., vol. 27, pp. 379–423, Jul.–Oct. 1948, 623–656.